Theoretical near UV and VIS electronic spectra for the Zn^{II}–anhydrotetracycline complex

Hélio F. Dos Santos,[a] Wagner B. De Almeida *[ab] and Michael C. Zerner [b]

[a] *LQC-MM: Laboratório de Química Computacional e Modelagem Molecular Depto. de Química, UFMG, Belo Horizonte, MG, 31270-901, Brazil*
[b] *QTP: Quantum Theory Project, University of Florida, Gainesville, FL 32611-8435, USA*

Received (in Gainesville, FL) 5th May 1998, Accepted 8th September 1998

The UV–VIS electronic spectra for the free ligand and complexed forms of the Zn^{II}–AHTC system have been analyzed using the configuration interaction (CI) procedure as implemented in the ZINDO program. The main transitions in the UV and VIS region are assigned and compared with the experimental data available. The electronic spectrum for the free ligand, the tautomeric form ionized at O^{11} [$LH^{-}(O^{11})$], is very close to that observed experimentally, with the calculated absorption band centered at 429 nm and the experimental one at 428 nm. This absorption is attributed to a $\pi\rightarrow\pi^*$ transition of the BCD ring system. Comparing the visible spectra for the complexed forms with that obtained for the free ligand, a blue shift is observed for all structures analyzed, except for the complex II-B, where a red shift from 429 nm (free ligand) to 436 nm (complexed form) was calculated. Experimentally, a bathochromic shift from 428 nm to 440 nm was observed with the [Zn^{II}]/[AHTC] ratio ranging from 0 to 3. These values are very close to those calculated for the complex II-B, in which the AHTC acts as a tridentate ligand. The possibility of the formation of the binuclear complex (M_2L) was discarded, once it was observed that the second metal complexation shifts the VIS band to lower wavelength values. This effect is not observed in the experimental spectrum at high Zn^{II} concentration.

Introduction

Tetracycline and its derivatives are widely used antibiotics that depress protein synthesis by blocking the aminoacyl-tRNA binding.[1] Like many other organic drugs, tetracyclines present several potential binding sites to metal ions. The antibacterial activity and adverse side effects associated with these compounds are related to the complexed form distribution.[2,3]

Considering the coordination properties of tetracyclines, the development of new and more active drugs requires that structural and energetic features of the complexation process be assigned beforehand. Toward this goal, experimental studies have been developed using different derivatives and metal ions.[3–11] In these studies, the main experimental techniques applied to access structure and metal coordination site are UV–VIS absorption spectroscopy and circular dichroism (CD). However, it has been pointed out that structural determination is complicated due to the coexistence of many species in solution, with different stoichiometries, and the difficulty in establishing the experimental conditions likely to favor the formation of a single complexed form.[7]

Recently we have carried out a series of studies involving the anhydrous derivative of tetracycline, 5a,6-anhydrotetracycline (hereafter called **AHTC**)[12–16] (Fig. 1). The free base[13] and complexed forms[14–16] of **AHTC** have been analyzed through quantum mechanical semiempirical methods. Our purpose in these investigations is to provide useful information regarding structure, conformational equilibrium and complexation. A theoretical investigation of the near UV and visible electronic spectra has also been done for the fully deprotonated form of **AHTC** compound[12] and the results showed a good agreement with the available experimental data.

In the present work, the calculated UV–VIS spectra have been used to analyze the possible coordination sites for the Zn^{II}–**AHTC** complex.

Calculation methodology

The complexation process involving **AHTC** and Zn^{II} was experimentally investigated at pH = 7.[11] From the study of the species distribution as a function of the pH for **AHTC**,[9,11] it was found that the main species present in the equilibrium at neutral pH is LH^{-} (Fig. 1). The conformational equilibrium for the **AHTC** molecule has been extensively investigated in our previous work.[13] In that study, all the ionized forms of **AHTC** were considered and the solvent effect was included through the continuous approach. The results showed that the LH^{-} ionized form is present in water solution as an *extended* conformation, with relative concentration estimated at 99%. This conformation was used in a comprehensive investigation of stationary points present on the potential energy surface (PES) for the Zn^{II}–**AHTC** complex.[14] All the possible coordination sites (shown in Fig. 1) were analyzed with complexation energies calculated in gas phase and simulated water solution.[14]

In this study, the UV–VIS electronic spectra for the free ligand LH^{-} ionized at O^{10} and O^{11} (Fig. 1) and the most probable

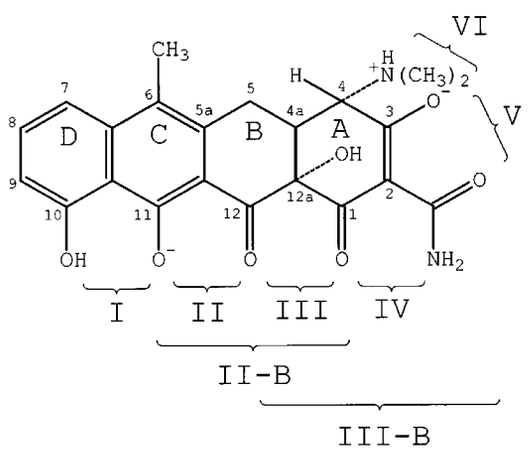

Fig. 1 Numbering scheme of the **AHTC** molecule and the possible metal complexation sites: I(O^{10}–O^{11}), II(O^{11}–O^{12}), II-B(O^{11}–O^{12}–O^{1}), III(O^{12}–O^{1}), III–B(O^{12}–O^{1}–O_{am}), IV(O^{1}–N_{am}), V(O^{3}–O_{am}) and VI(O^{3}–N^{4}).

Table 1 Calculated electronic transitions for the $LH^-(O^{10})$ and $LH^-(O^{11})$ ionized species of the **AHTC** molecule. The wavelength (λ/nm) and oscillator strengths (f) were calculated in the presence of the self consistent reaction field generated by water (SCRF, $\varepsilon = 78.54$)

λ	f	CI contribution [a]	λ_{max} [b]	ε_{max} [b]	Assignment [c]
$LH^-(O^{10})$					
374	0.31127	83% (79→82)	375	15 252	π→π* (BCD)
338	0.12293	79% (79→83)	338	11 030	π→π* (BCD)
278	0.17649	62% (76→82)	258	37 029	π→π* (ABCD)
268	0.02816	34% (78→82)			
257 [d]	0.20138	15% (81→91)			
257 [d]	0.22213	35% (80→91)			
257 [d]	0.15085	45% (81→91)			
215	0.40622	14% (76→83)	216	24 792	π→π* (BCD)
$LH^-(O^{11})$					
429	0.49572	74% (80→82)	429	24 294	π→π* (BCD)
264	0.21568	34% (80→86)	260	25 395	π→π* (ABCD)
263 [d]	0.10570	31% (81→89)			
257	0.05053	62% (80→90)			
256	0.06616	42% (76→83)			
256 [d]	0.04993	34% (74→87)			
222	0.26551	42% (80→91)	224	17 210	π→π* (BCD)

[a] Only the main CI contribution has been shown. The molecular orbital number 81 corresponds to the HOMO in both compounds. [b] λ_{max} (nm) and ε_{max} (dm^3 mol^{-1} cm^{-1}) are respectively the wavelength and the molar absorptivity obtained from the simulated spectra (Fig. 2). [c] The labels A to D stand for the ring chromophore system of the AHTC molecule. [d] These transitions contain contribution of the A ring.

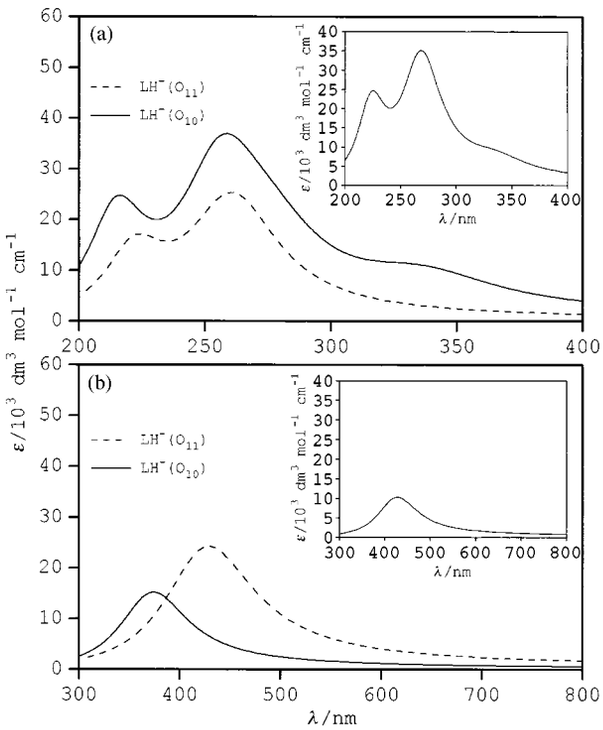

Fig. 2 (a) UV and (b) VIS calculated and experimental (inset) electronic spectra for the LH^- ionized form of the **AHTC** molecule.

complexed forms obtained from ref. 14 were calculated using the ZINDO program as parametrized by Zerner and coworkers.[17] The solvent effect was included in the calculation using the SCRF (self-consistent reaction field) ($\varepsilon = 78.54$) formulation as given by Karelson and Zerner [18] with the inclusion of the dipole and quadrupole term in the electrostatic potential expansion. The electronic spectra for the free ligand (LH^-) were obtained using a configuration interaction (CI) calculation including all single excitation from the 16 highest occupied molecular orbitals (MO) to the 16 lowest unoccupied MOs. A total of 257 configurations were generated. For the complexed forms (II, III, II-B, III-B, II/VI, III/VI and II-B/VI) an active space constituted of 36 occupied and 36 unoccupied MOs was used to generate 1297 configurations.

Results and discussion

The calculated UV and VIS electronic spectra, obtained in water solution (SCRF model; $\varepsilon = 78.5$), for the $LH^-(O^{10})$ and $LH^-(O^{11})$ ionized forms of the **AHTC** molecule are depicted in Fig. 2. The band spectra were constructed using the simulation procedure developed in our previous work.[12] The transitions considered in the band spectra simulation are shown in Table 1. From Fig. 2(a), it can be seen that the UV spectrum for the $LH^-(O^{10})$ species presents three absorption bands located at [λ_{max}/nm (ε_{max}/dm^3 mol^{-1} cm^{-1})]: 216 (24 800), 258 (37 000) and 338 (11 000). For the $LH^-(O^{11})$ deprotonated form, only two bands are observed in the UV region, centered at 224 and 260 nm, with intensities lower than those calculated for the O^{10} ionized species (see Table 1). For both compounds, the absorptions were assigned as π→π* transitions of the BCD chromophore system (Fig. 1), with a contribution of the A ring for the band located near 260 nm. The experimental spectrum [19] showed absorptions at 224, 269 and 336 nm (shoulder) with molar absorptivity equal to 20 000, 31 770 and 4 000 dm^3 mol^{-1} cm^{-1} respectively. Except for the shoulder at 336 nm, the band positions observed are close to those calculated for the $LH^-(O^{11})$ species. For the $LH^-(O^{10})$ species, the intensity of the band located at 338 nm is overestimated in comparison with experiment. This discrepancy can be attributed in part to the simulation procedure,[12] as can be observed from the value of ε_{max} obtained in the simulation of the isolated band at 338 nm ($\varepsilon_{max} = 6000$ dm^3 mol^{-1} cm^{-1}). The presence of a shoulder near 330 nm has been observed for the fully deprotonated form of **AHTC** [$L^{2-}(O^{10})$],[12] showing that this absorption might be a characteristic of the O^{10} ionized species. Experimental evidence of this conclusion has been obtained in the metal–**AHTC** complexation studies,[9–11] where the disappearance of the shoulder at 336 nm has been observed when the coordination occurs in the O^{11}–O^{12} site (see Fig. 1 for the numbering scheme). According to the experimental studies,[9–11,19] the second ionization of the **AHTC** molecule is attributed to the O^{10} phenolic proton. In our recent works,[13,14] it was observed that the O^{11} deprotonated form is 3.6 kcal mol^{-1} more stable than the O^{10} one in the gas phase and 4.2 kcal mol^{-1} in water solution (using the COSMO solvent model [20]). The available theoretical and experimental data suggest that both ionized forms might exist in aqueous medium. The tautomeric equilibrium is displaced to the $LH^-(O^{11})$ form in the presence of the metal, due to the complexation in the O^{11}–O^{12} coordination site.

In the VIS region, Fig. 2(b) shows only one absorption band located at 375 [$LH^-(O^{10})$] and 429 nm [$LH^-(O^{11})$], attributed to a transition of the π→π* molecular orbitals of the BCD ring system (Table 1). As in the UV region, the theoretical spectra show a red shift in this absorption due to the $LH^-(O^{10}) \rightleftharpoons LH^-(O^{11})$ tautomerization process. The experimental spectrum [11,19] exhibited a band at 428 nm, which is very close to the value calculated for the O^{11} ionized species. The intensity of this absorption (see Table 1) seems overestimated in relation to the experimental value ($\varepsilon_{max} = 10\,270$ dm^3 mol^{-1} cm^{-1}). A possible reason for this is the use of a constant width at half height in the simulation procedure.[12] The experimental band spectra obtained by applying the simulation procedure [12] to the experimental data [19] are shown in Fig. 2 (inset).

The absorption band in the VIS region has been considered important in characterizing the complexation reactions. Experimentally, the shift observed in that band is used to determine the coordination site.[9–11] In our previous work,[14] the potential energy surface (PES) for the Zn^{II}–**AHTC** interaction was comprehensively investigated using the semiempirical AM1 model. Table 2 gives the values of the free energy of complex-

Table 2 Relative free energy of complexation [$\Delta(\Delta G)$/kcal mol^{-1} calculated at 298 K] [$\Delta(\Delta G)$ calculated relative to the most stable structure] and Gibbs populations (in brackets) for the distinct tetrahedral complexes Zn^{II}–**AHTC** obtained in gas phase and aqueous solution[a]

	Complexation sites for MHL complex:[b] $[ZnLH(H_2O)_2]^+$ and $[ZnLH(H_2O)]^+$					
	II	III	II-A[c]	II-B	III-A[c]	III-B
$\Delta(\Delta G^{gas})$[d]	7.14 [0.0%]	3.08 [0.4%]	0.38 [32.4%]	0.00 [61.6%]	2.28 [1.3%]	1.58 [4.3%]
$\Delta(\Delta G_1^{aq})$[e]	16.9 [0.0%]	12.9 [0.0%]	10.2 [0.0%]	0.00 [93.1%]	11.6 [0.0%]	1.58 [6.9%]
$\Delta(\Delta G_2^{aq})$[f]	19.4 [0.0%]	13.6 [0.0%]	10.8 [0.0%]	0.46 [46.0%]	11.8 [0.0%]	0.00 [54.0%]
$\Delta(\Delta G_3^{aq})$[g]	0.58 [18.9%]	8.81 [0.0%]	18.9 [0.0%]	0.00 [50.3%]	20.5 [0.0%]	0.36 [27.4%]
	Complexation sites for M_2L complex:[b] $[Zn_2L(H_2O)_4]^{2+}$ and $[Zn_2L(H_2O)_3]^{2+}$					
	II/VI	III/VI	II-B/VI			
$\Delta(\Delta G^{gas})$[d]	0.00 [99.5%]	18.1 [0.0%]	14.8 [0.0%]			
$\Delta(\Delta G_1^{aq})$[e]	0.00 [99.5%]	18.1 [0.0%]	4.30 [0.0%]			
$\Delta(\Delta G_2^{aq})$[f]	15.7 [0.0%]	0.00 [100%]	5.72 [0.0%]			
$\Delta(\Delta G_3^{aq})$[g]	0.00 [98.8%]	15.4 [0.0%]	2.63 [1.2%]			

[a] From ref. 14. [b] The complexation sites are defined in Fig. 1. [c] Coordination number of Zn^{II} = 5. [d] $\Delta G^{gas} = \Delta H - T\Delta S + \Delta E + \Delta ZPE$. ($\Delta H - T\Delta S$) corresponds to the thermal correction to the Gibbs free energy of complexation, obtained from the vibrational, rotational and translational partition functions. ΔE and ΔZPE are the energy (electronic + nuclear) and the zero point energy of complexation respectively. [e] $\Delta G_1^{aq} = \Delta G^{gas} + \Delta E_1^{sol}$: $\Delta E_1^{sol} = -166\,(1 - 1/\varepsilon)q^2/a_0$, where ε = relative permittivity (= 78.5), q = net charge and a_0 = solute cavity radius = 0.732 $(m/\rho)^{1/3}$, being m the molecular mass and ρ the density (assumed to be 1 g cm^{-3}). [f] $\Delta G_2^{aq} = \Delta G_1^{aq} + \Delta E_2^{sol}$: $\Delta E_2^{sol} = -166\,[(2\varepsilon - 2)/(2\varepsilon + 1)](P_e^2/a_0^3)$, where P_e = dipole moment. The Onsager term has the inconvenience of origin dependence in the case of charged species. However, if a new origin is selected at $\mathbf{r}_0$ relative to the old point chosen as the origin of the molecular coordinates the new dipole moment (P_e') will be related to the old dipole (P_e) by the relationship $P_e' = P_e - q\mathbf{r}_0$ (see ref. 21). This will have no effect in our free energy results, since we are comparing relative energies of different isomers of the same molecule with respect to the same origin of the molecular coordinates. [g] $\Delta G_3^{aq} = \Delta G^{gas} + \Delta E^{sol}$(COSMO): ΔE^{sol}(COSMO) evaluated using the COSMO model for solvent effects (see refs. 14, 20).

ation obtained from the AM1 optimized structure of the distinct Zn^{II}–**AHTC** complexes. From the energy values and Gibbs population analysis, it can be seen that the geometry II-B, in which the **AHTC** is a tridentate ligand, was found to be the most stable structure for the complex MHL both in gas phase and water simulation, considering the ΔG_1 and ΔG_3 values. The inclusion of the dipole term (ΔG_2) in the solvent energy, showed that the complex III-B is 0.5 kcal mol^{-1} more stable than the structure II-B. For the bimetallic complexes (M_2L), the geometry II/VI was found to be the global minimum on the PES for the Zn^{II}–**AHTC** interaction both in the gas phase and water calculated according to the value of ΔG_1 and ΔG_3. However, the solvent effect evaluated from the ΔG_2 value, yields structure III/VI as favored by 16 kcal mol^{-1} in relation to II/VI. The calculations presented in Table 2 suggest that the first complexation should occur at the II-B or III-B site and the second one at site VI, with a change from II-B to II or from III-B to III. From these results, we decided to investigate the electronic spectra for the MHL complexes II, II-B, III and III-B and for the M_2L structures II/VI, II-B/VI and III/VI.

The positions (λ and f) and assignment of the main transitions observed for the complexed structures II, III, II-B and III-B are reported in Table 3. The UV and VIS band spectra are shown in Figs. 3(a) and 3(b) respectively.

For the structures where **AHTC** acts as a bidentate ligand (II and III) the main absorptions in the UV region are attributed to the $\pi \rightarrow \pi^*$ transition centered on the BCD ring system. The transitions from the MO of the A ring were located at 284, 261, 258 nm (II) and 278 nm (III) with f equal to 0.136, 0.127, 0.378 and 0.151 respectively. Although complex III presents the metal coordinated to O^1 (a carbonyl oxygen of the A ring), no characteristic transitions involving the molecular orbital located in the A ring were calculated. However, two new transitions centered at 375 and 311 nm were calculated for structure III with moderated intensities (Table 3) and assigned as a $\pi \rightarrow \pi^*$ excitation of the BCD chromophore.

As in the case of structure II, the electronic transitions calculated for II-B are mainly from the BCD rings. Transitions involving molecular orbitals from the A ring were calculated at 260 and 234 nm, the former more intense (f = 0.404). For the complex III-B, in which the amide group is involved in the

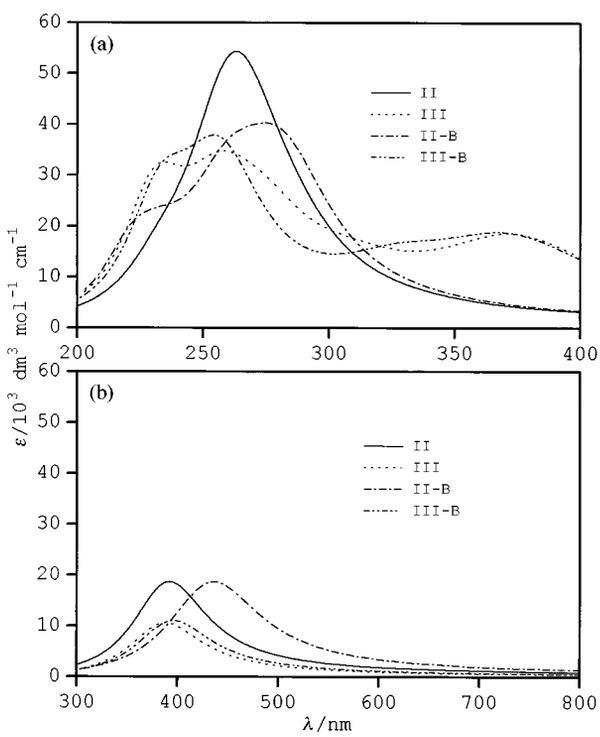

Fig. 3 (a) UV and (b) VIS electronic spectra for the distinct Zn^{II}–**AHTC** tetrahedral complexes.

metal coordination *via* the oxygen atom (Fig. 1), the main transitions in the UV region came from the A ring (Table 3). An absorption at 374 nm was calculated for the III-B structure. This transition is located in the same region as observed for complex III, so it seems that this absorption is a characteristic of the coordination involving the O^{12}–O^1 moiety (site III).

Examining Fig. 3(a) and Table 3, we see that the electronic spectrum for structure II contains a broad band centered at 263 nm, due to the two intense transitions calculated at 266 nm (f = 0.531) and 258 nm (f = 0.378). For complex II-B, the simulated spectrum showed an absorption band centered at 275 nm which consists of transitions calculated at 282 nm (f = 0.549)

Table 3 Theoretical electronic spectra for the tetrahedral Zn^{II}–**AHTC** complexes. The wavelength (λ) and the oscillator strengths (f) were calculated in water solution considering the SCRF model ($\varepsilon = 78.54$). The λ_{max} (nm) and ε_{max} ($dm^3\ mol^{-1}\ cm^{-1}$) were obtained from the simulated band spectra

II (O^{11}–O^{12})[a]			III (O^{12}–O^{1})[a]				II-B (O^{11}–O^{12}–O^{1})[a]			III-B (O^{12}–O^{1}–O_{am})[a]			
λ/nm	f	Main CI contribution[b]	λ/nm	f	Main CI contribution[b]	Assignment[c]	λ/nm	f	Main CI contribution[b]	λ/nm	f	Main CI contribution[b]	Assignment[c]
392	0.382	90% (89→90)	388	0.217	42% (89→90)	π→π* (BCD)	436	0.382	92% (85→86)	396	0.226	44% (85→86)	π→π* (BCD)
			375	0.294	49% (89→90)	π→π* (BCD)				374	0.276	37% (85→86)	π→π* (BCD)
			311	0.106	58% (89→91)	π→π* (BCD)				327	0.146	40% (84→87)	π→π* (A)
284	0.136	37% (88→92)	278	0.151	37% (88→92)	π→π* (A)	282	0.549	26% (85→87)				π→π* (BCD)
266	0.531	37% (87→90)	272	0.108	13% (87→90)	π→π* (BCD)	260	0.404	21% (84→88)	263	0.103	52% (84→89)	π→π* (A)
261	0.127	25% (88→94)				π→π* (A)	234	0.137	85% (84→91)	256	0.485	28% (84→89)	π→π* (A)
258	0.378	18% (88→94)				π→π* (A)	222	0.223	26% (81→87)	233	0.430	42% (83→88)	π→π* (BCD)
			257	0.376	31% (89→93)	π→π* (BCD)							
233	0.128	45% (87→91)	231	0.473	35% (87→91)	π→π* (BCD)							
λ_{max}		ε_{max}	λ_{max}		ε_{max}	Assignment[c]	λ_{max}		ε_{max}	λ_{max}		ε_{max}	Assignment[c]
392		18 721	388		10 634	π→π* (BCD)	436		18 719	396		11 073	π→π* (BCD)
			372		18 610	π→π* (BCD)				368		18 894	π→π* (BCD)
263		54 397	258		34 808	π→π* (ABCD)	275		40 358	254		37 974	π→π* (ABCD)
			235		32 604	π→π* (BCD)	229		23 224	237		33 938	π→π* (BCD)

[a] See Fig. 1 for the numbering scheme. [b] Only the main CI contribution has been considered. The molecular orbital 89 corresponds to the HOMO for the II and III structures and 85 is the HOMO for the II-B and III-B species. [c] The labels A, B, C and D stand for the rings of the AHTC molecule (Fig. 1).

and 260 nm ($f = 0.404$). The shoulder at 229 nm for structure II-B was not observed for complex II, due to the low intensity of the transition at 233 nm ($f = 0.128$). For the complexed forms III and III-B three absorption bands are calculated in the UV region with λ_{max} predicted at 372, 258 and 235 nm (shoulder) (III) and 368, 254 and 237 nm (shoulder) (III-B). As mentioned above, the band near 375 nm is observed only for structures that contain the metal coordinated to site III. This absorption might be used by the experimentalists as a reference for coordination involving the O^{12} and O^{1} atoms. Comparing the UV spectra of the free ligand with those of the complexed forms a bathochromic shift is observed near to 260 nm when the coordination occurs at sites II and II-B accompanied with an increase of intensity. The same red shift was observed for the absorption band close to 220 nm. For structures III and III-B, a blue shift is obtained for the transition near 260 nm and a red shift for the absorption close to 220 nm. As in the case of the non-complexed form of **AHTC**, the UV absorptions for all structures analyzed were assigned as $\pi \rightarrow \pi^*$ transition of the BCD chromophore, with contribution of the A ring for the absorption bands near 260 nm. In all complexed forms, the contribution from the A ring involves an electronic transition from the molecular orbital HOMO-1, which is concentrated on the amide group. The transitions related with the A ring for the free form of the **AHTC** molecule were found at 257 nm [$LH^-(O^{10})$] and 263 nm [$LH^-(O^{11})$], and consist of three nearly degenerated transitions centered at 257 nm with significant oscillator strength for the O^{10} deprotonated form. As opposed to the metal complexed forms, these transitions came from the HOMO, which is composed of atomic orbitals centered at the amide group.

An important aspect of the UV spectra is the disappearance of the shoulder near 330 nm. According to our previous discussion, this absorption should be observed only for the O^{10} ionized species. In this work, we consider the tautomeric form ionized at the O^{11} phenolic oxygen for all the complexation reactions. The coordination sites II and II-B involve the O^{11} moiety, so the ligand should be present in the $LH^-(O^{11})$ tautomeric form in those complexes. For structure III, there are two possible ionized species. The theoretical results show that the complex III ionized at O^{10} is 19 kcal mol^{-1} higher in energy than the corresponding O^{11} deprotonated structure. As expected, the calculated UV spectrum of the complex III ionized at O^{10} has an absorption at 336 nm with oscillator strength equal to 0.04. Experimentally, no data have been reported for the absorption spectra in the 200–300 nm region for the Zn^{II}–**AHTC** complex.

Due to the presence of many chiral centers, the CD spectrum has been considered to be the most useful technique in the conformational analysis and coordination sites determination involving tetracycline derivatives. The experimental UV absorption spectra are not discussed in detail in the majority of the studies reported. The reasons for this can be related to the difficulty of the assignment and correlation of the absorption band with structural aspects. Regarding the UV spectra for the Zn^{II}–**AHTC** complexes shown in this study, it can be seen that this spectral region presents some characteristic absorption that can be useful for the identification of the coordination site. Therefore, we believe that the theoretical results can guide the experimentalists in the analysis of the complexation process involving tetracyclines and also stimulate them to re-examine the experimental spectra.

The lowest energy transitions are calculated at 392 (II), 388 (III), 436 (II-B) and 396 nm (III-B) (Table 3). The calculated spectra are displayed in Fig. 3(b). The results presented in Table 3 show that the greatest wavelength is calculated for the structure which the metal ion coordinated to the II-B site ($\lambda = 436$ nm). Experimentally,[11] a bathochromic shift has been observed from 428 to 440 nm followed by a decrease of the intensity when the molar ratio [Zn^{II}]/[AHTC] changes from 0 to 3. The theoretical results show a hypsochromic shift of the VIS

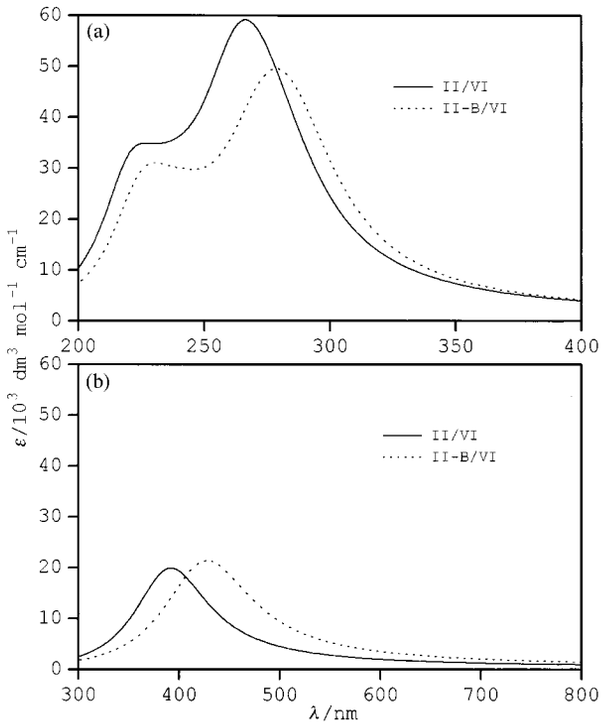

Fig. 4 (a) UV and (b) VIS electronic spectra for the bimetallic complexes II/VI and II-B/VI.

absorption band for structures II and III and III-B, when compared with the spectrum for the free ligand $LH^-(O^{11})$. Based on the experimental work,[11] it was proposed that the metal ion (Zn^{II}) coordinates to the O^{11} and O^{12} groups (site II, Fig. 1), yielding the MHL species. In that same study, it was suggested that the **AHTC** probably acts as a tridentate system due to the high value of the complex formation constant obtained.[11] As mentioned before, the disappearance of the shoulder near 330 nm may be an indication of the complexation at sites II or II-B (involving the O^{11} atom). However, the coordination site III and III-B should also be considered, since the calculations suggest that the O^{11} ionized form of III is more stable than the corresponding O^{10} tautomer. The values of the VIS transitions reported in Table 3 indicate that the greatest wavelength is calculated for structure II-B, suggesting that this coordination site is the most probable one if the absorptions relative to the $LH^-(O^{11})$ are considered as reference. For that complex, the calculated shift is from 429 nm [$LH^-(O^{11})$] to 436 nm (II-B). The decrease in the intensity observed (Tables 1 and 3) is also in agreement with the experimental data.[11] From these results and those published previously,[14] we conclude that the Zn^{II}–**AHTC** complex, with a single metal coordinated to the ligand (MHL), should be present in solution as structure II-B, in agreement with the experimental proposal.

The possibility of the formation of a bimetallic complex (M_2L) has been considered, through the coordination of a second Zn^{II} ion to the N^4 and O^3 position on the A ring (site VI, Fig. 1). Fig. 4 shows the calculated UV [4(a)] and VIS [4(b)] electronic spectra for the tetrahedral structures II/VI and II-B/VI. The band spectra were obtained from the calculated values of λ and f presented in Table 4. It can be seen in Fig. 4 that the UV region consists of two transitions centered at 227 (shoulder) and 267 nm (II/VI) and 230 (shoulder) and 279 nm (II-B/VI), representing a hypsochromic and a bathochromic shift when the absorptions of structure II-B/VI are compared with the corresponding bands of the II/VI complex. A small red shift relative to MHL (structures II and II-B) is observed in the calculated results for both compounds, due to the complexation at site VI. As for the other structures investigated, the shoulder near 330 nm was not observed for those compounds. The UV bands are attributed to a $\pi \rightarrow \pi^*$ transition of the BCD rings,

Table 4 Theoretical electronic spectra for the bimetallic complexes (M_2L). The wavelength (λ) and oscillator strengths (f) were calculated in water solution (SCRF model; $\varepsilon = 78.54$)

II/VI (O^{11}–O^{12}/N^4–O^3)[a]			II-B/VI (O^{11}–O^{12}–O^1/N^4–O^3)[a]			
λ/nm	f	CI contribution[b]	λ/nm	f	CI contribution[b]	Assignment[c]
392	0.407	88% (97→98)	428	0.437	88% (93→94)	π→π* (BCD)
279	0.301	64% (96→99)	285	0.453	53% (91→95)	π→π* (A)
265	0.873	31% (95→98)	275	0.514	23% (93→96)	π→π* (BCD)
237	0.177	40% (95→100)	242	0.175	32% (92→96)	π→π* (BCD)
221	0.450	61% (94→100)	225	0.299	36% (90→96)	π→π* (BCD)

λ_{max}[d]/nm	ε_{max}[d]/dm^3 mol^{-1} cm^{-1}	λ_{max}[d]/nm	ε_{max}[d]/dm^3 mol^{-1} cm^{-1}	Assignment[c]
392	19 946	428	21 414	π→π* (BCD)
267	59 213	279	49 599	π→π* (ABCD)
227	34 912	230	31 093	π→π* (BCD)

[a] See Fig. 1 for the numbering scheme. [b] Only the main CI contribution has been considered. The molecular orbitals number 97 and 93 correspond to the HOMO for the II/VI and II-B/VI complexes respectively. [c] The labels A, B, C and D stand for the rings of the AHTC molecule (Fig. 1). [d] λ_{max} and ε_{max} are respectively the wavelength and molar absorptivity obtained from the simulated spectra (Fig. 4).

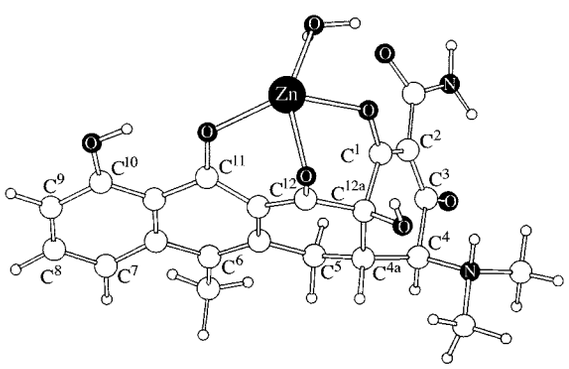

Fig. 5 AM1 optimized structure of the tridentate complex [ZnLH-$(H_2O)]^+$ (II-B).

with a contribution of the A ring for the absorption near to 260 nm. The CI contributions reported in Table 4, show that the absorption band at 279 nm in the simulated spectra for structure II-B/VI contains a significant contribution from the A ring, located at 285 nm ($f = 0.453$). For structure II/VI, the absorption involving the A ring was calculated at 279 nm ($f = 0.301$) and is assigned as a transition from the HOMO−1 to LUMO+1. As for the complexes II, II-B, III and III-B, the transitions related with the A ring has a participation of a molecular orbital constituted by atomic orbitals centered at the amide group.

In the VIS region of the electronic spectra only one transition is calculated for both structures centered at 392 (II/VI) and 428 nm (II-B/VI) respectively [Fig. 4(b)]. The absorptions were assigned as a π→π* (HOMO→LUMO) transition of the BCD chromophore. For structure II/VI, the band position and intensity are calculated to be close to the value obtained for complexes II. The VIS electronic spectrum for the complexed form II-B/VI presents an absorption band close to the value observed for the free ligand ($\lambda_{max} = 428$ nm). Regarding structure II-B, a blue shift from 436 nm (II-B) to 428 nm (II-B/VI) is calculated when the second metal coordinates to the **AHTC** molecule. The values obtained from the calculated UV–VIS electronic spectra for structure III/VI are not reported in Table 4 and Fig. 4. The reason is that the previous analysis for the MHL species showed that the complex III should not be observed in the medium. The lowest energy transition for the complex III/VI was calculated at 388 nm ($f = 0.060$), which is the same value calculated for structure III (Table 3).

From the experimental analysis of the species distribution against the total metal concentration,[11] it was concluded that the MHL and M_2L species are both likely to be present in the medium when the [Zn^{II}]/[AHTC] ratio is about 3. The results obtained in the present work show that complexation at site VI (O^3–N^4) should shift the visible absorption band to a lower wavelength. As this effect is not observed in the experimental spectrum, we conclude that the main species present in aqueous solution at pH 7 for the Zn^{II} and **AHTC** system is structure II-B, with only one metal ion coordinated at the O^{11}–O^{12}–O^1 moiety. The AM1 optimized structure[14] of the complex Zn^{II}–**AHTC** (II-B) is shown in Fig. 5.

Finally, it is important to mention that the methodology applied in the present study was able to identify the correct coordination site for the Zn^{II}–**AHTC** complexation process. Studies are underway on other metal–**AHTC** complexes (Al^{III}[15] and Mg^{II}[16]), in order to establish a solid base for the use of calculation of the electronic spectra to analyze the structure of **AHTC** complexation.

Conclusions

A theoretical electronic spectra analysis is made to investigate the possible coordination sites of the Zn^{II}–**AHTC** system. The free ligand and different complexed forms were analyzed and the changes in the UV–VIS electronic spectra compared with the available experimental data.

For the free ligand we find that the O^{11} ionized form [LH^--(O^{11})] is more likely to be present in water solution at pH 7. The VIS absorption band was calculated at 429 nm to be comparable to the experimental value of 428 nm. From a thermodynamic point of view, the O^{11} deprotonated form was also found to be 4 kcal mol^{-1} more stable than the O^{10} one in water solution, in agreement with our conclusion based on spectra alone.

We further examine the MHL and M_2L species. From these calculations, we observed a blue shift, in the absorption band for structures II, III, III-B, II/VI, III/VI and II-B/VI relative to the free ligand LH^-(O^{11}). Only for complex II-B do we calculate a bathochromic shift from 429 nm [LH^-(O^{11})] to 436 nm (II-B). The experimental spectrum shows a red shift from 428 nm (free ligand) to 440 nm when the molar ratio [Zn^{II}]/[AHTC] is equal to 3. From these results we conclude that the main species present in aqueous solution for the Zn^{II}–**AHTC** system is structure II-B, where the metal ion is coordinated to the O^{11}–O^{12}–O^1 moiety and the **AHTC** molecule acts as a tridentate ligand.

Acknowledgements

W. B. D. A. would like to thank the Fundação Coordenação de Aperfeiçoamento de Pessoal de Nível Superior (CAPES) for a research grant and also the Fundação de Amparo a Pesquisa do Estado de Minas Gerais (FAPEMIG) and the Programa de Apoio ao desenvolvimento Científico e Tecno-

lógico (PADCT-Proc. No. 62.0241/95.0) for partially supporting this project. H. F. D. S. thanks the Conselho Nacional de Desenvolvimento Científico e Tecnológico (CNPq) for a research grant. This work was supported in part through grants from the office of Naval Research and through NSF grant CHE 9312651.

References

1 D. Voet and J. G. Voet, *Biochemistry*, 2nd end., John Wiley & Sons, Inc., New York, USA, 1995.
2 A. I. Laskin and J. A. Last, *Antibiot. Chemother.*, 1971, **17**, 1.
3 L. Lambs and G. Berthon, *Inorg. Chim. Acta*, 1988, **151**, 33.
4 W. A. Baker, Jr. and P. M. Brown, *J. Am. Chem. Soc.*, 1966, **88**, 1314.
5 K. H. Jogun and J. J. Stezowski, *J. Am. Chem. Soc.*, 1976, **98**, 6018.
6 G. W. Everett, Jr., J. Gulbis and J. Shaw, *J. Am. Chem. Soc.*, 1982, **104**, 445.
7 L. Lambs, B. D.-Le Révérend, H. Kozlowski and G. Berthon, *Inorg. Chem.*, 1988, **27**, 3001.
8 M. Jezowska-Bojczuk, L. Lambs, H. Kozlowski and G. Berthon, *Inorg. Chem.*, 1993, **32**, 428.
9 J. M. De Siqueira, S. Carvalho, E. B. Paniago, L. Tosi and H. Beraldo, *J. Pharm. Sci.*, 1994, **83**, 291.
10 F. C. Machado, C. Demicheli, A. Garnier-Suillerot and H. Beraldo, *J. Inorg. Biochem.*, 1995, **60**, 163.
11 S. V. De Mello-Matos and H. Beraldo, *J. Braz. Chem. Soc.*, 1995, **6**, 405.
12 W. B. De Almeida, L. R. A. Costa, H. F. Dos Santos and M. C. Zerner, *J. Chem. Soc.*, *Perkin Trans. 2*, 1997, 1335.
13 H. F. Dos Santos, W. B. De Almeida and M. C. Zerner, *J. Pharm. Sci.*, 1998, **87**, 190.
14 W. B. De Almeida, H. F. Dos Santos, W. R. Rocha and M. C. Zerner, *J. Chem. Soc.*, *Dalton Trans.*, 1998, **15**, 2531.
15 W. B. De Almeida, H. F. Dos Santos and M. C. Zerner, *J. Pharm. Sci.*, 1998, **87**, 1101.
16 W. B. De Almeida, H. F. Dos Santos and M. C. Zerner, to be published.
17 (*a*) J. Ridley and M. C. Zerner, *Theor. Chim. Acta*, 1973, **32**, 111; (*b*) M. C. Zerner, G. H. Loew, R. F. Kirchner and V. T. Mueller-Westerholf, *J. Am. Chem. Soc.*, 1980, **102**, 589; (*c*) J. D. Head and M. C. Zerner, *Chem. Phys. Lett.*, 1986, **131**, 359; (*d*) W. D. Edwalds and M. C. Zerner, *Theor. Chim. Acta*, 1987, **72**, 347.
18 M. M. Karelson and M. C. Zerner, *J. Phys. Chem.*, 1992, **96**, 6949.
19 J. M. Siqueira, MSc Thesis, Depto. de Química, UFMG, 1989.
20 A. Klamt and G. Schuurmann, *J. Chem. Soc.*, *Perkin Trans. 2*, 1993, 799.
21 A. Hinchliffe and R. W. Munn, *Molecular Electromagnetism*, John Wiley & Sons, Chichester, 1985.

Paper 8/03419B